Springer

KSME

Journal of Mechanical Science and Technology 31 (5) (2017) 2287~2294
www.springerlink.com/content/1738-494x(Print)/1976-3824(Online)
DOI 10.1007/s12206-017-0425-5

An immersed-boundary method for conjugate heat transfer analysis †

Jeong Chul Song[1], Joon Ahn[2,*] and Joon Sik Lee[1]

[1]*School of Mechanical & Aerospace Engineering, Seoul National University, Seoul 151-742, Korea*
[2]*School of Mechanical Engineering, Kookmin University, 136-702 Seoul, Korea*

(Manuscript Received July 6, 2016; Revised December 8, 2016; Accepted December 26, 2016)

Abstract

An immersed-boundary method is proposed for the analysis of conjugate problems of convective heat transfer in conducting solids. Inside the solid body, momentum forcing is applied to set the velocity to zero. A thermal conductivity ratio and a heat capacity ratio, between the solid body and the fluid, are introduced so that the energy equation is reduced to the heat diffusion equation. At the solid fluid interface, an effective conductivity is introduced to satisfy the heat flux continuity. The effective thermal conductivity is obtained by considering the heat balance at the interface or by using a harmonic mean formulation. The method is first validated against the analytic solution to the heat transfer problem in a fully developed laminar channel flow with conducting solid walls. Then it is applied to a laminar channel flow with a heated, block-shaped obstacle to show its validity for geometry with sharp edges. Finally the validation for a curvilinear solid body is accomplished with a laminar flow through arrayed cylinders.

Keywords: Immersed-boundary method; Conjugate heat transfer; Effective thermal conductivity

1. Introduction

In engineering problems involving convective heat transfer, flows are usually in the turbulent regime. For turbulent convection, because turbulent heat flux is dominant over thermal diffusion, most previous studies have not considered heat conduction inside solid walls or in obstacles in the flow path [1]. However, heat transfer in the laminar regime is influenced by thermal boundary conditions such as isothermal wall or iso-heat flux wall. Moreover, in the turbulent regime where large variations in local heat transfer occur, the temperature distribution inside a solid body strongly affects convective heat transfer characteristics [2]. Then heat transfer characteristics can substantially be changed from the case with an isothermal or iso-heat flux wall.

A large number of previous works on convective heat transfer are focused on the development of heat transfer enhancement devices such as turbulence promoters, serpentine passages, impinging jets and so forth. Local heat transfer in those devices is spatially varied. Large variations in local heat transfer generate conduction inside a solid wall, so that the heat transfer is affected. In addition, recent research interest is moving to heat transfer in micro-structures, where flows are usually in the laminar regime. Thus, conduction in the solid wall should be considered as well as convection in the flow for more accurate evaluation of heat transfer rates in practical applications.

Previous numerical studies on conjugate heat transfer were mainly carried out for laminar flow [3-7], or considered only a steady-state formulation of the governing equations [8]. Various numerical procedures have been used for conjugate heat transfer analysis. One of the numerical methods is the domain decomposition procedure [6]. In this procedure, the solid region is decomposed from the fluid region, each region is calculated separately, and then the boundary values at the solid fluid interface are matched to satisfy the boundary conditions. This approach has good accuracy for the prediction of conjugate heat transfer. It has problems, however, such as slow convergence and difficulty in applying this approach to complex geometry or three-dimensional flow paths. What is worse is that it causes low accuracy in heat transfer prediction when the solid body has a sharp edge, like a rectangular rib.

To overcome these disadvantages, a unitary computational domain has been used in some previous studies [4, 5, 7]. This approach sets the velocity inside a solid body to zero by imposing high artificial viscosity and satisfies the continuity of the heat flux at the solid fluid interface using the harmonic mean or the concept of effective conductivity. This approach does not need the iteration for matching boundary conditions between the solid region and the fluid region. Therefore, it can be more easily applied to complex geometry as well as to three-dimensional problems and also can improve the slow convergence. In spite of these advantages, this approach has

*Corresponding author. Tel.: +82 2 910 4833, Fax.: +82 2 910 4839
E-mail address: jahn@kookmin.ac.kr
† Recommended by Associate Editor Jungil Lee

an accuracy problem when the velocity gradient is very large at the solid fluid interface. This is a result of the artificial manipulation which does not set the velocity at the solid fluid interface to zero.

Another approach using a unitary computational domain is finite element formulation [3]. In this formulation, the Galerkin method of weighted residuals is used to discretize the non-linear system of governing equations and boundary conditions. The computational domain is divided into a set of non-overlapping regions, termed elements, in which the dependent variables are approximated with interpolation functions in terms of the local normalized element coordinates. Substitution of the approximations into the system of governing equations and boundary conditions yields a residual for the conservation equations. These residuals are reduced to zero in a weighted sense over each element volume by making them orthogonal to the interpolation functions. The discrete representation for the entire computational domain is obtained through an assembly of those elemental equations. This procedure can easily satisfy the change in boundary conditions at the solid fluid interface and can also improve the slow convergence. In addition, it can be easily applied to complex geometry and three-dimensional problems. However, the procedure needs a determination of the proper weight function for interpolation and domain of influence, which considerably affect the accuracy of the solution.

Some previous studies conducted simulations for heat transfer analysis based on the immersed-boundary method [9]. Kim and Choi [10] have suggested the immersed-boundary method for convective heat transfer analysis when the solid wall has iso-thermal or iso-heat flux conditions. Kang et al. [11] presented a novel immersed-boundary method for multi-material heat transfer problems. In this method, two approximated boundaries facing each other across the solid fluid interface are constructed to build connections between points on the two approximated boundaries.

In this paper, we propose a numerical technique based on the immersed-boundary method to analyze the conjugate heat transfer problem. In the immersed-boundary method, a solid body in the flow field is considered as a kind of momentum forcing in the Navier-Stokes equations rather than the real body, and thus, the flow over a complex geometry can be easily handled with orthogonal (Cartesian) grids which generally do not coincide with the solid surface [9]. On the other hand, by applying the immersed-boundary method to the conjugate heat transfer problem, we can deal with both the fluid region and the solid region in a unitary computational domain. In general, momentum forcing is imposed not only on the solid fluid interface but also inside solid body to ensure the stability of the method at a high Reynolds number. This procedure sets the velocity in the solid region to zero so that the energy equation is reduced to the heat diffusion equation by assigning thermal conductivity to the solid region. In the case of complex geometry, some cells in the computational domain span the solid and fluid regions because the solid fluid interface does not generally coincide with the grids. We resolve such cells by introducing an effective thermal conductivity [4, 5, 7] and by modifying convection terms.

The immersed boundary method proposed by Kang et al. [11] applies heat source to have the targeted value of temperature at the nodal points near the solid-fluid interface. The temperature is obtained by mapping and interpolation to satisfy the heat flux continuity. The procedure is parallel to that of the momentum forcing. But the interpolation factor for the temperature should be different from that for the velocity to consider fluxes at both sides of the interface separately. This mismatch can affect the boundness of temperature depending on the mesh refinement. On the other hand, the present numerical procedure of treating the energy equation is not exactly parallel to that of the momentum forcing. However, the stability is less affected by the mesh refinement.

In this study, three different laminar flow problems are simulated to verify the accuracy of our method. We first validate the method against the analytic solution of the heat transfer problem in a fully developed laminar channel flow with conducting solid walls and observe the accuracy depending on the mesh refinement. Next we conducted numerical simulations for a laminar channel flow with a heated rectangular obstacle and a laminar flow through an array of cylinders to compare our simulation results to previously published data [3, 6] in order to confirm accuracy of our heat transfer prediction near the sharp corner of the solid body and the validity of the solution for the curvilinear solid body in a Cartesian grid system.

2. Numerical method

2.1 Governing equation

In this study, we use the incompressible Navier-Stokes equation and the energy equation. The dimensionless continuity and momentum equations can be expressed as

$$\frac{\partial u_i}{\partial x_i} = 0 \tag{1}$$

$$\frac{\partial u_i}{\partial t} + \frac{\partial u_i u_j}{\partial x_j} = -\frac{\partial p}{\partial x_i} + \frac{1}{\mathrm{Re}}\frac{\partial^2 u_i}{\partial x_j \partial x_j} \tag{2}$$

where x_i are the Cartesian coordinates, u_i are the corresponding velocity components, p is the pressure and Re is the Reynolds number. To satisfy the no-slip condition at the solid fluid interface, we apply both momentum forcing (f_i) and mass source/sink (ms) on the solid surface. Momentum forcing is imposed inside the solid body to set the velocity to zero. The modified continuity and momentum equations are expressed as

$$\frac{\partial u_i}{\partial x_i} - ms = 0 \tag{3}$$

$$\frac{\partial u_i}{\partial t} + \frac{\partial u_i u_j}{\partial x_j} = -\frac{\partial p}{\partial x_i} + \frac{1}{\mathrm{Re}}\frac{\partial^2 u_i}{\partial x_j \partial x_j} + f_i \, . \tag{4}$$

The method of determining momentum forcing (f_i) and mass source/sink (ms) is fully described in Kim et al. [9].

In the case of a thermal field, the dimensionless energy equation can be expressed as

$$\frac{\partial\theta}{\partial t}+\frac{\partial\left(u_j\theta\right)}{\partial x_j}=\frac{1}{\mathrm{Re}\,\mathrm{Pr}}\frac{\partial^2\theta}{\partial x_j\partial x_j} \tag{5}$$

where θ is the dimensionless temperature and Pr is the Prandtl number. No-slip condition on the solid surface and zero velocity inside the solid body are satisfied by introducing momentum forcing and mass source/sink so that the energy equation inside the solid body is reduced to the heat diffusion equation.

Considering thermal property variation and energy balance across the solid fluid interface, Eq. (5) can be written as

$$\frac{\partial\theta}{\partial t}+\omega\frac{\partial\left(u_j\theta\right)}{\partial x_j}=\frac{C^*K^*}{\mathrm{Re}\,\mathrm{Pr}}\frac{\partial^2\theta}{\partial x_j\partial x_j}+\xi\,. \tag{6}$$

The difference in thermal properties between the solid and the fluid is reflected in the energy equation by introducing the heat capacity ratio C^* and the thermal conductivity ratio K^*.

Those are set to unity in the fluid region and become $(\rho c_p)_f/(\rho c_p)_s$ and k_s/k_f inside the solid body, where $(\ )_f$ and $(\ )_s$ indicate the properties of the fluid and the solid. Heat capacity at the cell including the interface is evaluated as the weighted volume average over the cell. Thermal conductivity at the cell face, however, needs an additional treatment to satisfy the heat flux continuity at the interface. The procedure is given in Sec. 2.2. In Eq. (6), ω is a convective correction factor. ω is used to take into account conduction at the solid fluid interface independently. Its value is zero in the cells at the interface and solid region, while it becomes unity for other cells. ξ is a kind of heat source/sink, which is introduced to compensate for error generated by neglecting the convection effect at the interface. Its definition is given in Sec. 2.3.

2.2 Effective thermal conductivity

When we apply the immersed-boundary method to a conjugate heat transfer problem, the conduction inside the solid body is solved by imposing momentum forcing inside the solid body. Momentum forcing sets the velocity to zero so that the energy equation becomes the heat diffusion equation. The remaining issues are continuity of temperature and conservation of energy at the solid fluid interface. In this study, we introduce the concept of effective thermal conductivity to satisfy the continuity of temperature and conservation of energy at the interface. Effective thermal conductivity is determined according to the arrangement of the solid fluid interface and the direction of heat flux at the interface as shown in Fig. 1. When the heat flux crosses the interface (see Fig. 1(a)), i.e. the phase at neighboring cell centers are different, the effective conductivity (k_e) at the interface is defined as

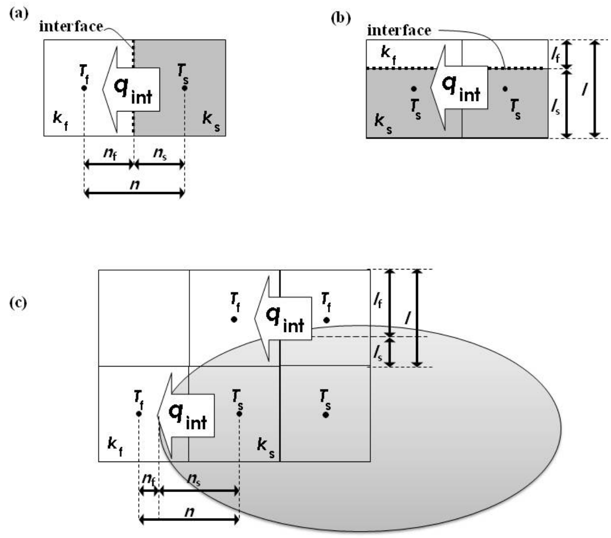

Fig. 1. Heat flux at the solid-fluid interface for (a) heat flux normal to the cell face; (b) heat flux parallel to the cell face; (c) general geometry.

$$q_{\mathrm{int}}=-k_e\frac{T_f-T_s}{n}\,. \tag{7}$$

At the interface, the temperature and heat flux should be continuous. It follows that

$$T_{\mathrm{int}}\big|_f=T_{\mathrm{int}}\big|_s \tag{8}$$

$$k_s\left.\frac{\partial T}{\partial n}\right|_s=k_f\left.\frac{\partial T}{\partial n}\right|_f\,. \tag{9}$$

Canceling out the interface temperature in Eqs. (8) and (9), and plugging in Eq. (7), the effective thermal conductivity can be expressed as [7]

$$\frac{k_e}{k_f}=\frac{(k_s/k_f)n}{(k_s/k_f)n_f+n_s}\,. \tag{10}$$

On the other hand, when the heat flux does not cross the interface as shown in Fig. 1(b), i.e. the phase at the cell center does not change for the neighboring cell, the effective conductivity is determined from a weighted average value as given by Eq. (11).

$$K^*=\frac{k_e}{k_f}=\frac{1}{l}\int\frac{k(l)}{k_f}dl\,. \tag{11}$$

A general case is illustrated in Fig. 1(c).

2.3 Convection in cells including the interface

When the cell face coincides with the solid fluid interface, there is no convection in the cell inside the solid body faced

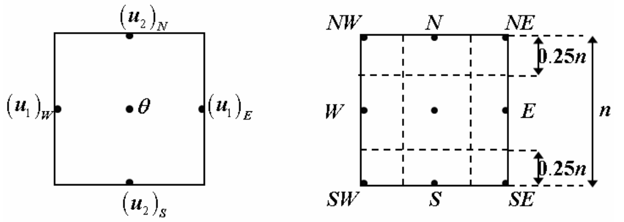

Fig. 2. Interpolation points to evaluate the convective correction term.

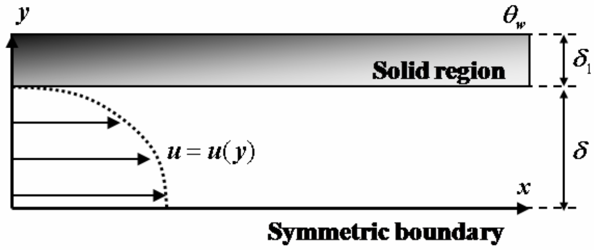

Fig. 3. Channel with a conducting wall.

with the interface so that ξ, as a kind of heat source/sink, becomes zero. However, if the cell face does not coincide with the interface, we should consider the convection to get more accurate result. Convection in the cells including the interface is treated by imposing heat source/sink to satisfy the energy conservation, which is similar to how the mass source/sink satisfies the mass conservation at the interface [9]. In the capacity of heat source/sink, ξ is defined as

$$\xi = -\frac{1}{\Delta V}\sum_i \mathbf{u}_{\mathrm{f}}\,\theta\cdot\mathbf{n}\,\Delta n_{\mathrm{f},i}\ . \tag{12}$$

In the study, we determine enthalpy flux through interpolation (see Fig. 2) using the fluid area ($\Delta n_{\mathrm{f},j}$) in the cell to get higher accuracy, differing from Kim et al. [9]. The interpolation relation is given by

$$(u_{\mathrm{f}}\theta)_{\mathrm{W}} = 0.25(u\theta)_{\mathrm{NW}} + 0.5(u\theta)_{\mathrm{W}} + 0.25(u\theta)_{\mathrm{SW}}\,. \tag{13}$$

The treatment improves numerical stability for a coarse grid.

3. Code verification

3.1 Laminar channel flow with conducting solid wall

The proposed numerical method is validated against the conjugate heat transfer in a laminar channel flow (see Fig. 3) by comparing it with the analytic solution. For a fully developed flow with iso-heat flux boundary condition, the axial temperature gradient becomes constant. Thus, temperature can be decomposed as

$$\theta = \frac{d\theta_b}{dx}x + \tilde{\theta}\ . \tag{14}$$

So that Eq. (5) can be modified as [10]

Table 1. Simulation conditions and mesh refinement for channel flow with a conducting wall.

Simulation conditions		Mesh refinement	
		Number of grid	Grid spacing ($\Delta y/\delta$)
Re	1000	256	7.81×10^{-3}
Pr	0.71	128	1.56×10^{-2}
δ_1/δ	1.0	64	3.13×10^{-2}
k_s/k_f	10, 100	32	6.25×10^{-2}

$$u\frac{d\theta_b}{dx} = \frac{1}{\mathrm{Re\,Pr}}\frac{d^2\tilde{\theta}_{\mathrm{f}}}{dy^2}\ . \tag{15}$$

In the solid region, Eq. (15) becomes

$$\frac{d^2\tilde{\theta}_{\mathrm{f}}}{dy^2} = 0\ . \tag{16}$$

The boundary conditions to Eqs. (15) and (16) are given by

$$\theta_f\big|_{u=\delta} = \theta_{\mathrm{int}},\ \frac{\partial\theta_f}{\partial y}\bigg|_{y=\delta} = 0 \tag{17}$$

$$T_{\mathrm{s}}\big|_{y=\delta} = T_{\mathrm{int}}\ ,\ T_{\mathrm{s}}\big|_{y=\delta+\delta_1} = T_{\mathrm{w}}\ . \tag{18}$$

The analytic solutions to Eqs. (15) and (16) can easily be obtained by substituting conditions at the interface given by Eqs. (8) and (9) as follows.

$$\frac{\theta_{\mathrm{f}}-\theta_{\mathrm{int}}}{1-\theta_{\mathrm{int}}} = \frac{3}{2}K^*\frac{\delta}{\delta_1}\left\{\frac{1}{2}\left(\frac{y}{\delta}\right)^2 - \frac{1}{12}\left(\frac{y}{\delta}\right)^4 - \frac{5}{12}\right\} \tag{19}$$

$$\frac{\theta_{\mathrm{s}}-\theta_{\mathrm{int}}}{1-\theta_{\mathrm{int}}} = \frac{\delta}{\delta_1}\left(\frac{y}{\delta}-1\right). \tag{20}$$

Simulations are performed for thermal conductivity ratios of 10 and 100 when the δ_1/δ = 1.0 and Re = 1000. The simulation conditions and grid information are listed in Table 1. Fig. 4 shows local temperature distributions. As can be seen in Fig. 4, the present numerical solutions faithfully follow the analytic solutions for both thermal conductivity ratios. Fig. 5 shows the variation of errors in temperature with mesh refinement. It is verified that the present numerical method has second-order accuracy in space.

3.2 Laminar channel flow with a heated obstacle

We conducted numerical simulations for a laminar channel flow with a heated rectangular obstacle as shown in Fig. 6 to see the effect of the thermal conductivity ratio of solid to fluid as well as to validate the accuracy of the present numerical method. Our results are compared to Young and Vafai's data [3] obtained by the finite element formulation. In this formula-

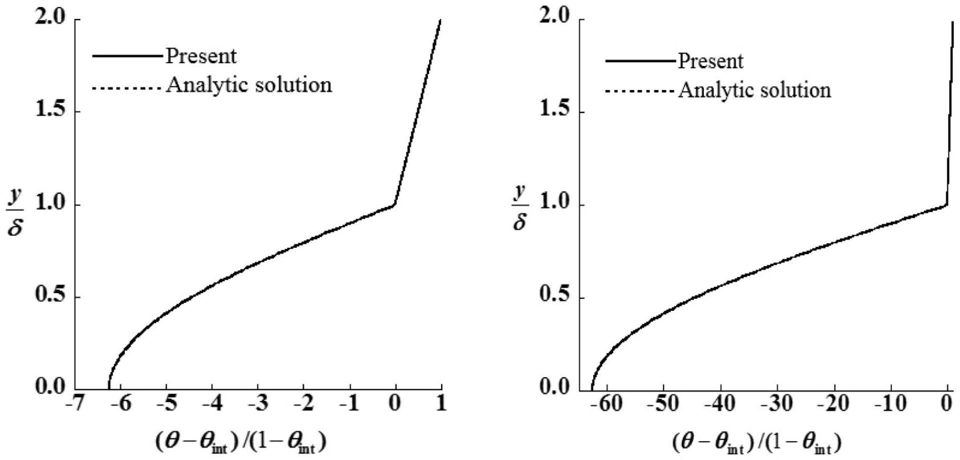

(a) (b)

Fig. 4. Temperature profiles in the channel with a conducting wall in comparison to the analytic solution: (a) $k_s/k_f = 10$; (b) $k_s/k_f = 100$.

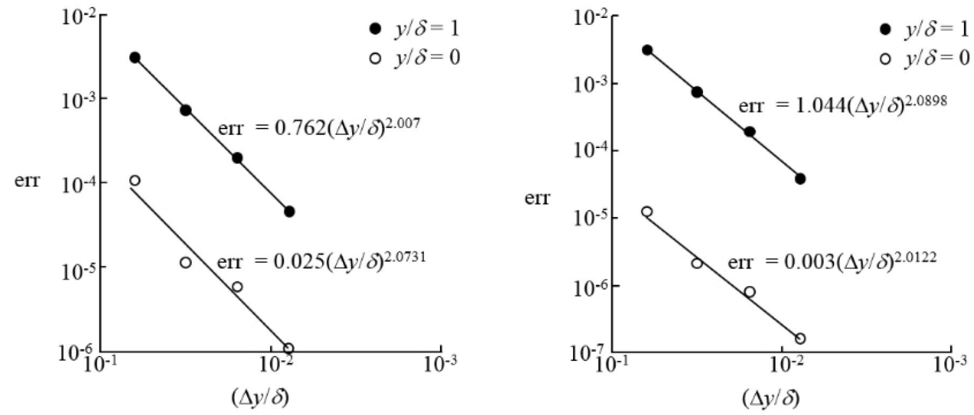

(a) (b)

Fig. 5. Numerical accuracy in temperature with mesh refinement: (a) $k_s/k_f = 10$; (b) $k_s/k_f = 100$.

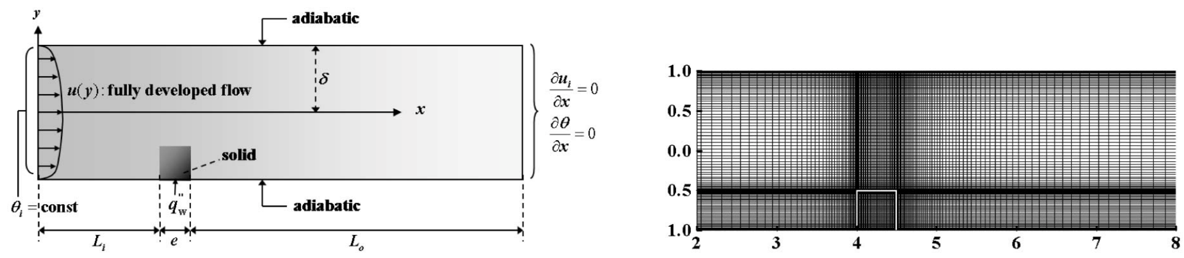

(a) (b)

Fig. 6. Channel with a heated obstacle: (a) Computational domain and boundary conditions; (b) grid system.

tion, the Galerkin method of weighted residuals of the finite element formulation is used to discretize the nonlinear system of governing equations and boundary conditions. The continuum domain is divided into a set of non overlap regions, termed elements, and the dependent variables within each element are approximated using interpolation functions in terms of the local normalized element coordinates.

In this simulation, the dimensionless temperature is defined as

$$\theta \equiv \frac{T - T_i}{q''_w H / k_f} . \tag{21}$$

Simulation conditions are listed in Table 2. At the channel inlet, flow is fully developed and temperature is constant ($\theta_i = 0$), and at the channel outlet, zero streamwise gradients are prescribed. Both the upper and lower channel walls are insulated except at the obstacle location. The base of the solid

Table 2. Simulation conditions for channel flow with a heated obstacle.

e/δ	0.5
L_i/δ	4
L_o/δ	16
Re	1000
Pr	0.71
k_s/k_f	10, 100

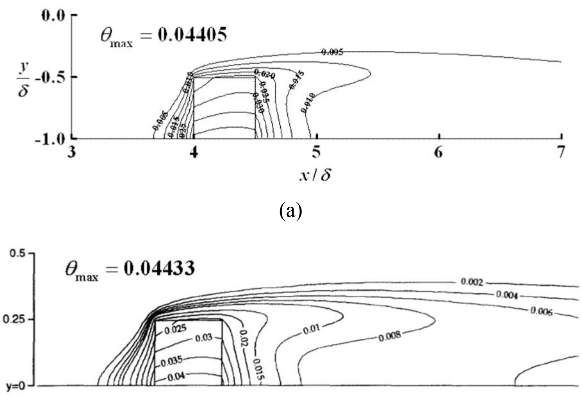

(a)

(b)

Fig. 7. Temperature contours in the case of k_s/k_f = 10: (a) This study; (b) Young and Vafai [3].

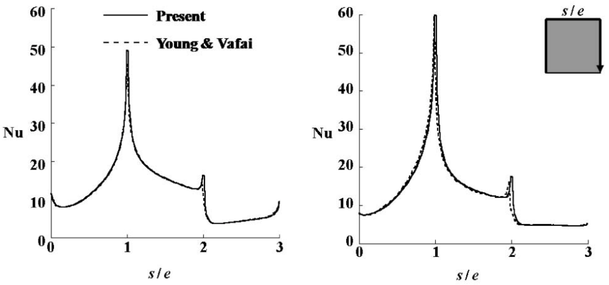

(a)

(b)

Fig. 8. Local Nusselt number distributions: (a) k_s/k_f = 10; (b) k_s/k_f = 100.

obstacle receives the iso-heat-flux ($q_w^{"}$). Simulations are performed for thermal conductivity ratios of 10 and 100. We use 128 × 96 meshes in the streamwise direction (x) and wall-normal direction (y). A non uniform grid system is used in both directions (Fig. 6(b)).

Fig. 7 shows the temperature contour in the case of $k_s / k_f = 10$ which is similar to that predicted by Young and Vafai [3]. A comparison of the maximum temperature with that predicted by Young and Vafai is within ~0.6 %. Fig. 8 shows the local Nusselt number distributions along the obstacle surface. The convective heat transfer coefficient and the Nusselt number are defined as

$$h = \frac{q_w^{"}}{T_{int} - T_i}, \quad \mathrm{Nu} = \frac{hD_h}{k_f}. \tag{22}$$

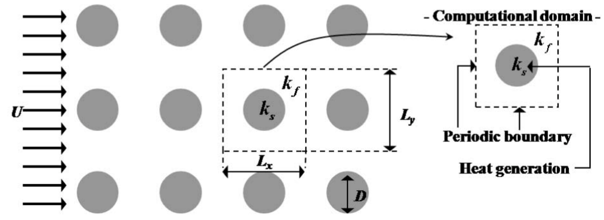

Fig. 9. Laminar flow across a cylindrical fin array with internal heating.

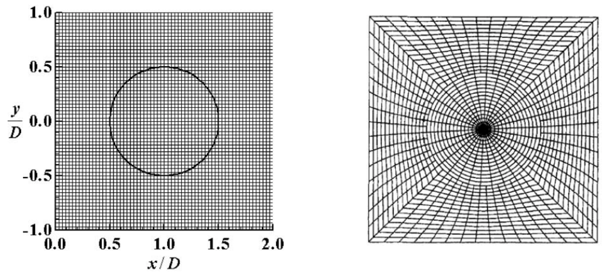

(a)

(b)

Fig. 10. Grid system for the periodic computational domain: (a) Cartesian coordinates used in this study; (b) polar coordinates used by Wang and Georgiadis [6].

As can be seen in Fig. 7, our predictions coincide almost exactly with Young and Vafai's [3] for both thermal conductivity ratios.

3.3 Flow over a cylinder array

In order to verify that the present method can predict conjugate heat transfer for curved geometry such as a cylindrical body, we conducted numerical simulations for laminar flow over a cylinder array with volumetric heating as shown in Fig. 9. Simulation results are compared to Wang and Georgiadis's data obtained by domain decomposition procedure [6]. In the procedure, the solid region is decomposed from the fluid region, each region is calculated separately and then the boundary values at the solid fluid interface are matched to satisfy the boundary conditions. The governing equations are solved for curvilinear coordinates, as shown in Fig. 10(b). We simulate the conjugate heat transfer on Cartesian coordinates (Fig. 10(a)). Simulation conditions are listed in Table 3. Four boundaries (inlet, outlet, top and bottom) have periodic boundary conditions.

Uniform volumetric heat (q_s) is generated inside the cylindrical solid body. In this simulation, the temperature is decomposed into a linear component and a periodic component as shown in Eq. (14) in order to satisfy the periodic condition in the streamwise direction. The temperature in dimensionless form is defined as

$$\theta \equiv \frac{\tilde{T} - \tilde{T}_b}{q_s \pi D^2 / 4k_f}. \tag{23}$$

Table 3. Simulation conditions for cross-flow over a cylinder array with internal heating.

L_x/D	2
L_y/D	2
Re	100
k_s/k_f	1, 100

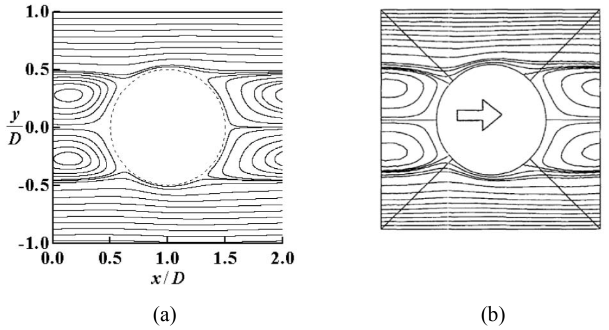

Fig. 11. Streamlines of the periodic flow at Re = 100: (a) This study; (b) Wang and Georgiadis [6].

Fig. 11 shows the streamlines together with the numerical results of Wang and Georgiadis [6]. In Fig. 11(a), flow recirculation is observed and flow parallels the streamwise direction near $y/D \approx \pm 1$. These characteristics are similar to those of Wang and Georgiadis (Fig. 11(b)). Temperature contours are shown in Fig. 12. Fig. 12(a) shows that the temperature inside the cylindrical solid body is almost uniform and most of the change in temperature occurs in the fluid region near the solid body. In addition, the fluid absorbs heat from the solid body so that the temperature increases in the streamwise direction. This thermal field predicted by our numerical method is also almost identical to that of Wang and Georgiadis (Fig. 12(b)).

The effect of convection can be quantified by examining the distribution of the local temperature gradient. The dimensional temperature gradient presented by and Wang and Georgiadis [6] is related to the dimensionless temperature gradient predicted by the present method as follows.

$$\frac{\partial T}{\partial n} = \frac{\pi D q_s}{4k_f}\frac{\partial \theta}{\partial N} \tag{24}$$

$$\frac{\pi D q_s}{4k_f} = \int_0^{2\pi} -\frac{k_f}{2}\frac{\partial T}{\partial n} d\phi . \tag{25}$$

Fig. 13 shows the dimensionless local temperature gradient compared to that of Wang and Georgiadis [6]. As seen in Fig. 13, the present result coincides almost exactly with that of Wang and Georgiadis [6]. Finally we compare the average Nusselt number to Wang and Georgiadis's data, where the heat transfer coefficient h is defined by the following relation.

$$\frac{\pi D^2 q_s}{4} = \pi D h\left(\tilde{T}_{\max} - \tilde{T}_{\min}\right) \tag{26}$$

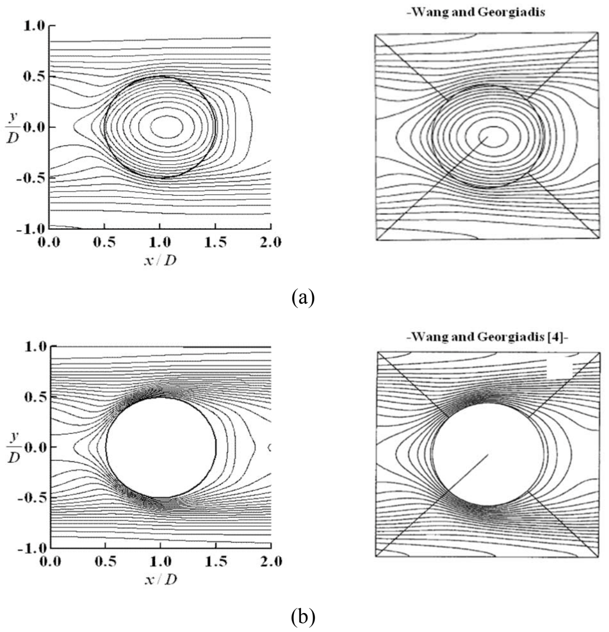

Fig. 12. Temperature contours for K_s = 100 at Re = 100: (a) k_s/k_f = 1: Contours from -0.02 to 0.17 by increment of 0.01; (b) k_s/k_f = 100: Contours from -0.02 to 0.08 by increment of 0.005.

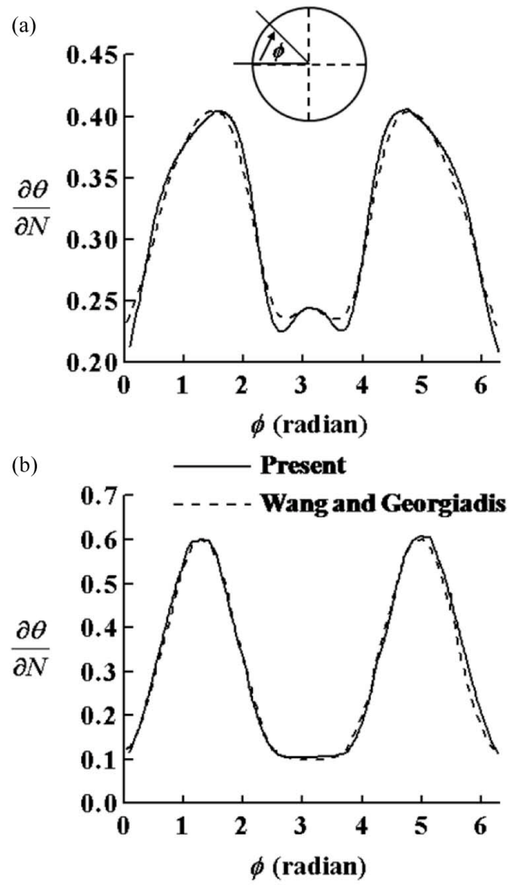

Fig. 13. Distribution of the local temperature gradient on the surface of a cylinder: (a) k_s/k_f = 1; (b) k_s/k_f = 100.

Table 4. Average Nusselt numbers on the surface of the cylinder.

k_s/k_f	Nu_{avg}		% error
	Present	Ref. [6]	
1	1.608	1.543	4.19
100	3.106	3.171	2.05

and the average Nusselt number is given by

$$Nu_{avg} = \frac{hD}{k_f} = \frac{D^2 q_s}{4k_f(\tilde{T}_{max} - \tilde{T}_{min})} = \frac{1}{\pi(\theta_{max} - \theta_{min})} . \quad (27)$$

The values of the averaged Nusselt numbers are listed in Table 4. The results show good agreement within 5 %.

4. Conclusions

In this study, an immersed-boundary method for conjugate heat transfer analysis is proposed. Momentum forcing is applied inside the solid wall to set the velocity to zero. A thermal conductivity ratio and heat capacity ratio between the solid body and the fluid are introduced so that the energy equation is reduced to the heat diffusion equation. At the solid fluid interface, heat flux continuity is satisfied by introducing effective thermal conductivity and a convective correction factor.

Our method has been validated for three different conjugate heat transfer problems, i.e., a channel flow with conducting solid wall, a channel flow with a heated, rectangular obstacle, and a flow through a conducting cylinder array. The simulation results agree well with the analytic solution and previous numerical results, proving the accuracy of the present numerical method. Each result verifies the accurate heat transfer prediction near the sharp corner of the solid body and on a curvilinear surface in a Cartesian grid system. The method will be applied to engineering problems with turbulent flows as a future work.

Acknowledgment

This research was supported by the 2013 Research Program (No. 20132010500060) of the Korea Institute of Energy Technology Evaluation and Planning (KETEP), funded by the Ministry of Trade, Industry & Energy, Republic of Korea.

References

[1] K. Fukagata, K. Iwamoto and N. Kasagi, Contribution of Reynolds stress distribution to the skin friction in wall-bounded flows, *Phys. Fluids*, 14 (2002) L73-L76.

[2] B. W. Webb and S. Ramadhyani, Conjugate heat transfer in a channel with staggered ribs, *Int. J. Heat Mass Transf.*, 28 (1985) 1679-1687.

[3] T. J. Young and K. Vafai, Convective cooling of a heated obstacle in a channel, *Int. J. Heat Mass Transf.*, 41 (1998) 3131-3148.

[4] C. W. Leung, S. Chen and T. L. Chan, Numerical simulation of laminar forced convection in an air-cooled horizontal printed circuit board assembly, *Numerical Heat Transf. Part A*, 37 (2000) 373-393.

[5] J. M. House, C. Beckermann and T. F. Smith, Effect of a centered conducting body on natural convection - convective heat transfer - in an enclosure, *Numerical Heat Transf. Part A*, 18 (1990) 213-225.

[6] M. Wang and J. G. Georgiadis, Conjugate forced convection in crossflow over a cylinder array with volumetric heating, *Int. J. Heat Mass Transf.*, 39 (1996) 1351-1361.

[7] N. O. Moraga and C. H. Salinas, Numerical model for heat and fluid flow in food freezing, *Numerical Heat Transf. Part A*, 35 (1999) 495-517.

[8] G. Iaccarino, A. Ooi, P. A. Durbin and M. Behnia, Conjugate heat transfer predictions in two dimensional ribbed passages, *Int. J. Heat Fluid Flow*, 23 (2002) 340-345.

[9] J. Kim, D. Kim and H. Choi, An immersed boundary finite volume method for simulation of flow in complex geometries, *J. Comput. Physics,* 171 (2001) 132-150.

[10] J. Kim and H. Choi, An immersed boundary finite volume method for simulation of heat transfer in complex geometries, *KSME Int. J.*, 18 (2004) 1026-1035.

[11] S. Kang, G. Iaccarino and F. Ham, DNS of buoyancy-dominated turbulent flows on a bluff body using the immersed boundary method, *J. Comput. Physics*, 228 (2009) 3189-3208.

[12] W. M. Kays and M. E. Crawford, *Convective heat and mass transfer*, 3rd ed., McGraw Hill, 108-158.

Joon Ahn received his B.S. (1997), M.S. (1999) and Ph.D. (2003) degrees from Seoul National University, Korea. He worked as a Senior Researcher at KIER (2006−2010) and is now a Professor at Kookmin University. His research interests include heat transfer and combustion problems in energy systems.